Jurnal Teknologi

Full Paper

OPTIMAL DESIGN OF A DYNAMIC VIBRATION ABSORBER BASED ON THE MODIFIED CAMEL ALGORITHM AND PHYSICAL CONCEPTS

Teeb Basim Abbas[a,b], Salwan Obaid Waheed Khafajib[c*]

[a]Air Conditioning and Refrigeration Techniques Engineering Department, Al-Mustaqbal University, 51001 Hillah, Babil, Iraq
[b]Department of Medical Instrumentation Techniques, College of Engineering and Information Technology, AlShaab University, Baghdad, Iraq
[c]Mechanical Power Technical Engineering Department, College of Engineering and Technologies, Al-Mustaqbal Energy Research Center, Al-Mustaqbal University, 51001, Babylon, Iraq

Article history
Received
2 July 2024
Received in revised form
7 September 2025
Accepted
7 September 2025
Published Online
16 June 2026

*Corresponding author
salwan.obaid@uomus.edu.iq

Graphical abstract

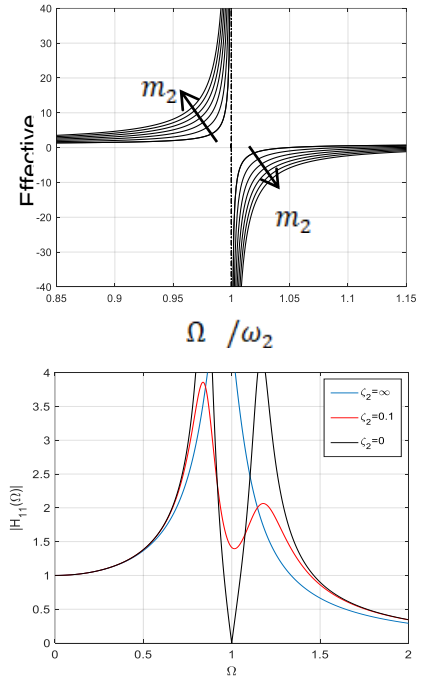

Abstract

This study provides an optimal design of a dynamic vibration absorber used for vibration attenuation for a wide range of real world applications. Principles of negative mass and stiffness are adopted and explained in detail in the mathematical modeling. Then, harmonic analysis is used to obtain the dynamic response of the absorber in terms of main system amplitude and resonance frequency. Based on the dynamic response, the modified Camel algorithm is used to obtain the optimal values of absorber in terms of some properties, damping and mass ratio. For several mass ratio scenarios, the ideal damping and frequency ratios are concurrently established. The results showed that damping ratios are very critical and important factors, even for a very small uncertainty. Damping by adding DVA changed the nonlinear harmonic response. The critical values of both damping ratio and frequency ratio must be carefully chosen because they are not independent. But when the frequency ratio increase, the behavior changes. Reducing the amplitude response by 400% involved increasing the DR from (0.1 to 0.4). Changes in the mass ratio and frequency have no effect on the amplitude response when $\Omega < 0.25$. The response is only impacted by frequency ratio in the range of ($0.5< \Omega <1.5$). Finally, the modified camel algorithm successfully, precisely, and economically determined the optimal design of the critical design parameters of the absorber. The optimal values of the design parameters are compared to some available method in literature and the results are more satisfied and precisely predicte.

Keywords: Absorber, optimal design, camel algorithm, negative stiffness, negative mass

© 2026 Penerbit UTM Press. All rights reserved

1.0 INTRODUCTION

A great deal of useful devices have been available for years. Because of their effectiveness, durability, and affordability, dynamic vibration absorbers (DVA) are among the most popular vibration control tools. Since the first DVA was created in 1909 by Frahm [1-2]. Traditionally, an undamped DVA include a mass

and a spring attached to a secondary vibrating system that vibrates in a narrowband frequency range. Numerous studies on and optimisation design [3–7] and absorber tuning [8–12] have been accomplished. A few of the aforementioned studies primarily focus on the beneficial effects of springs. An additional notion regarding negative stiffness was presented. In deformed objects, negative stiffness indicates the reversal of the force-displacement relationship. In dynamic vibration absorbers, negative stiffness elements act to counter these excitations through opposite reaction forces to external disturbances. The fundamental principle behind this is to tune the absorber for shunning the undesired vibrations within the particular frequency band. Research reports on the stability requirements of the negative stiffness (NS) can be found in References [13–19]. In addition to having a lower natural frequency, the NS system can support a greater load than the system with only positive stiffness. [20] created NS around equilibrium by utilising beams buckling under effect of an axial load, and by merge them with a linear positive spring. According to [21], who proposed a new vibration isolation system in which active control technique was used to achieve NS. NS principle was also applied to vibration isolation. [22] conducted both analytical and experimental research on a passive DVA with an NS mechanism. Additionally, [23] developed a nonlinear isolator with NS mechanism. When design parameters vary in value, the analytical solutions that are currently available for optimal parameters are time-consuming, have limited application, and are invalid [24]. Though the use of NS in vibration isolation systems has been the subject of extensive research due to its advantages, little has been written about the ideal DVA with NS and negative mass (NM) parameters in detail. Negative mass is an imagined ability of matter to behave as if an increase in force results in a decrease in acceleration. For dynamic vibration absorbers, negative mass produces a stronger response of the system to vibrations. If incorporated in an absorber, it can produce a force in opposition with the system to control it effectively in suppressing vibrations, which reduces the vibration amplitude of the system.

An additional crucial consideration is the optimal design of a DVA. The optimization techniques used in the best-designed system can generally be divided into (i) Den Hartog (DH) techniques, (ii) the gradient-based (GB) technique; and (iii) the global techniques [25]. The GB optimization methodology holds significant importance. The steepest decent algorithm approach was used by [26], [27], and [28] to solve their tuned mass damper (TMD) optimisation formulation. The gradient matrix of the objective function was derived by Hoang and Warnitchai (2005)[29], who then applied the Davidon–Fletcher–Powell to get the best possible solution. The most recent and possibly most effective technique for resolving limited nonlinear optimisation issues is sequential quadratic programming Rao, 1996 [30]. This technique has been used by numerous researchers recently to produce the ideal TMD design. Although gradient-based optimisation techniques are capable of precisely identifying local optimum points, they typically lack a mechanism for locating global optimum points. The best TMD system design parameters have been identified by using global optimisation techniques, particularly stochastic-based optimisation algorithms. Hadi and Arfiadi in (1998)[31] employed the genetic algorithm (GA), while Febbo and Vera in (2008) [32] employed the simulated annealing (SA) technique. It should be mentioned that there are other numerical techniques that can be found in published articles. For example, Park and Reed in (2001) [33] developed an algorithm for finding the best DTMD design. Optimization techniques can be computationally complex, sensitive to initial conditions, and struggle to converge to optimal solutions. They may also have limited applicability to certain dynamic vibration absorber systems and require expertise in numerical methods and algorithms, making them less accessible to non-experts. These issues can impact their reliability and applicability. In addition, the analytical methods for determining optimal parameters are time-consuming and are invalid when design parameters have a range of values. [34, 35] used the modified camel algorithm to obtain the optimal design of several engineering applications. They concluded that this technique is a robust, offering global optimization, fast convergence speed, adaptability, and ease of implementation.

This work presents the physical concept and detailed principles of negative mass and stiffness. In order to obtain the best combination for the secondary system parameters, the modified camel algorithm will be explained and used for optimization purposes.

2.0 METHODOLOGY

A. Negative Effective Mass

A system exposed to a harmonic excitation is depicted in Figure 1. The following represent the equations of motion for the frequency response functions (FRFs) H_{11} and H_{22} between the input harmonic force F(t) and the responses u_1(t) and u_2(t):

$$\begin{bmatrix} m_1 & 0 \\ 0 & m_2 \end{bmatrix}\begin{Bmatrix} \ddot{u}_1 \\ \ddot{u}_2 \end{Bmatrix}+\begin{bmatrix} k_1 & -k_1 \\ -k_1 & k_1 \end{bmatrix}\begin{Bmatrix} u_1 \\ u_2 \end{Bmatrix}=\begin{Bmatrix} F \\ 0 \end{Bmatrix}$$

$$F = F_o e^{j\Omega t}, \begin{Bmatrix} u_1 \\ u_2 \end{Bmatrix} = \begin{Bmatrix} a_1 \\ a_2 \end{Bmatrix} e^{j\Omega t}$$

$$\text{If n} = 1\ ,\ H_{n1} \equiv \frac{a_1}{F_o} = \frac{k_1 - m_2\Omega^2}{\left(k_1 - m_1\Omega^2\right)\left(k_1 - m_2\Omega^2\right) - k_1^2} \qquad (1)$$

If n =2, $H_{n1} \equiv \frac{a_k}{F_o} = \frac{k_1}{\left(k_1 - m_1\Omega^2\right)\left(k_1 - m_2\Omega^2\right) - k_1^2}$

For more convenience, the following terms are simplified as:

$$\widetilde{m}_1 \equiv \frac{F}{\ddot{u}_1} = \frac{F_o}{-\Omega^2 a_1} = m_1 + \frac{m_2}{1 - \Omega^2/\omega_2^2}, \omega_2 \equiv \sqrt{\frac{k_1}{m_2}} \quad (2)$$

here the principal mass is denoted by m_1 and the absorber mass by m_2. The excitation harmonic forces at the principal mass are denoted by F. The degrees of freedom of the principal and absorber mass, respectively, are denoted by $u_1(t)$ and $u_2(t)$. t is the time, Ω and ω_2 are the excitation and the resonance frequency of the additional absorber, respectively, represented by mass m_2 and stiffness k_2. When calculating the effective mass, indicated by$(\widetilde{m}_1)$, the system shown in Figure 1 is treated as a 1-DOF rather than a 2-DOF.

Eqn (2) shows that when $|\widetilde{m}| \to \infty$:

$$H_{11} = u_1(t) = 0, F_o = -k_1 a_2 \quad (3)$$

$$F(t) = -k_1 u_2(t) = m_2 \ddot{u}_2(t) \quad (4)$$

In other words, the presence of spring K has neutralized the effect of the external force due to the inertia force of the absorber mass $(-m_2\ddot{u}_2)$, and this is a good place to start when implying that the principal time response is $u_1(t)$= 0. The fundamental idea behind using a vibration absorber to reduce vibration is this mass's zero response.

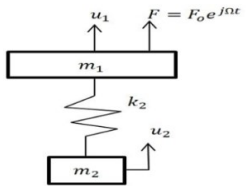

Figure 1 Mass-mass 2-DOF system

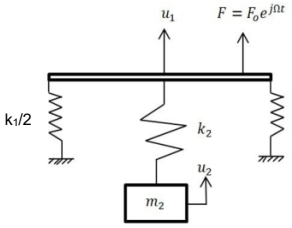

Figure 2 Spring-mass system with effective stiffness

B. Negative Effective Stiffness

Think about the 2D-O-F system shown in Figure 2. There are similarities between this system and Figure 1. On the left and right ends of the main mass, two subsprings, K_1, are added. The motion equations and their corresponding magnification factors $H_{n1}(\Omega)$ (n=1,2) are given by:

$$\begin{bmatrix} m_1 & 0 \\ 0 & m_2 \end{bmatrix} \begin{Bmatrix} \ddot{u}_1 \\ \ddot{u}_2 \end{Bmatrix} + \begin{bmatrix} k_1 + k_2 & -k_2 \\ -k_2 & k_2 \end{bmatrix} \begin{Bmatrix} u_1 \\ u_2 \end{Bmatrix} = \begin{Bmatrix} F \\ 0 \end{Bmatrix}$$

$$F = F_o e^{j\Omega t}, \begin{Bmatrix} u_1 \\ u_2 \end{Bmatrix} = \begin{Bmatrix} a_1 \\ a_2 \end{Bmatrix} e^{j\Omega t}$$

$$H_{11} \equiv \frac{a_1}{F_o} = \frac{k_2 - m_2\Omega^2}{\left(k_1 + k_2\right)\left(k_2 - m_1\Omega^2\right)\left(k_2 - m_2\Omega^2\right) - k_2^2} = \frac{1}{\widetilde{k}_1} \quad (5)$$

$$H_{21} \equiv \frac{a_2}{F_o} = \frac{k_2}{\left(k_1 + k_2\right)\left(k_2 - m_1\Omega^2\right)\left(k_2 - m_2\Omega^2\right) - k_2^2}$$

The following terms have been simplified for ease of use: $\widetilde{k}_1 \equiv \frac{F}{u_1} = \frac{F_o}{a_1} = k_1 + \frac{k_2}{1 - \omega_2^2/\Omega^2}, \omega_2 \equiv \sqrt{\frac{k_2}{m_2}}$ (6)

$\widetilde{k}_1$ is the effective spring.

When Ω= ω_2 $|\widetilde{k}_1| \to \infty$

and

$$H_{11} = u_1(t) = 0 \quad (7)$$

$$F(t) = -k_2 u_2(t) = m_2 \ddot{u}_2(t) \quad (8)$$

This essential indicates that since the spring is present, the absorber mass (–m2ü2) has neutralized the impact of the external force, and as a result, $u_1(t)$ a_2 =0. This also reveals that when, the term increases as m2 decreases. Even more crucially, the stiffness's effective value turns negative (NS) at both $\Omega < \omega_2$ and $k_2/(\omega_2^2/\Omega^2 - 1) > k_1$. According to this, a downward force developed and built up in the spring to reduce effect of the external force F(t), which can be given as:

$$F_o\left(\widetilde{k}_1 - k_1\right)/\widetilde{k}_1 = k_2\left(a_1 - a_2\right) \quad (9)$$

This force is bigger than the force $\Omega < \omega_2$ according to Eqn. (9). This conclusion clarifies the negative value of the stiffness.

Design an Absorber for Vibration Attenuation

Using Newton's second law, the governing differential equations of the physical system depicted in Figure 3 can be found as follows:

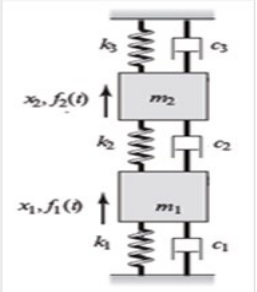

Fig. 3. Damped 2-DOF vibratory system

$$\begin{bmatrix} m_1 & 0 \\ 0 & m_2 \end{bmatrix}\begin{Bmatrix} \ddot{x}_1 \\ \ddot{x}_2 \end{Bmatrix}+\begin{bmatrix} c_1+c_2 & -c_2 \\ -c_2 & c_2+c_3 \end{bmatrix}\begin{Bmatrix} \dot{x}_1 \\ \dot{x}_2 \end{Bmatrix}+\begin{bmatrix} k_1+k_2 & -k_2 \\ -k_2 & k_2+k_3 \end{bmatrix}\begin{Bmatrix} x_1 \\ x_2 \end{Bmatrix}=\begin{Bmatrix} f_1 \\ f_2 \end{Bmatrix} \quad (10)$$

The force vector on the right side of Eqn. 10 is given by:

$$f_1(t)=F_1e^{j\omega t}, f_2(t)=F_2e^{j\omega t} \quad (11)$$

ω is the excitation frequency. The time response of Eqn (10) is given by:

$$x_i=X_i(j\omega)e^{j\omega t} \quad (12)$$

where i index are the system coordinates. The mathematical manipulation of Eqns (10), (11), and (12) results in more general form, so that:

Where

$$\begin{bmatrix} a_{11}(j\omega) & a_{12}(j\omega) \\ a_{21}(j\omega) & a_{22}(j\omega) \end{bmatrix}\begin{Bmatrix} X_1(j\omega) \\ X_2(j\omega) \end{Bmatrix}=\begin{bmatrix} F_1 \\ F_2 \end{bmatrix} \quad (13)$$

and

$$X_1(j\omega)=\frac{a_{22}(j\omega)F_1-a_{12}(j\omega)F_2}{D_o(j\omega)}$$
$$X_2(j\omega)=\frac{a_{11}(j\omega)F_2-a_{21}(j\omega)F_1}{D_o(j\omega)} \quad (14)$$

$$D_o(j\omega)=a_{11}(j\omega)a_{22}(j\omega)-a_{12}(j\omega)a_{21}(j\omega) \quad (15)$$

Effect of the force F_2 is neglected (F_2 =0) in this work to study effect of excitation force only on the response of the system in the presence of the DVA. So that Eqn. (14) can be updated as:

$$\lambda M_{11}(j\omega)=\lambda\frac{X_1(j\omega)}{F_1}=\lambda\frac{a_{22}(j\omega)}{D_o(j\omega)}$$
$$\lambda M_{21}(j\omega)=\lambda\frac{X_2(j\omega)}{F_1}=-\lambda\frac{a_{21}(j\omega)}{D_o(j\omega)} \quad (16)$$

$\lambda M_{11}(j\omega)$ and $\lambda M_{21}(j\omega)$ are the frequency responses functions. In order to eliminate the dimension, a non-dimensional parameter denoted by λ (N/m) was added. In this work, the other two frequency responses are not considered. The general form of the frequency response can be obtained by:

$$H_{ij}(j\omega)=\beta\left|M_{ij}(j\omega)\right| \quad i,j=1,2 \quad (17)$$

The two parameters denoted by $a_{ij}(j\omega)$ in Eqn. (13) can be given:

$$a_{11}(j\omega)=A(j\Omega)k_1, a_{12}(j\omega)=-B(j\Omega)k_1m_r$$
$$a_{21}(j\omega)=-B(j\Omega)k_1m_r, a_{22}(j\omega)=D(j\Omega)k_1m_r \quad (18)$$

where,

$$\Omega=\frac{\omega}{\omega_{n1}}\ \omega_r=\frac{\omega_{n2}}{\omega_{n1}}\ 2\zeta_i=\frac{c_i}{m_i\omega_{ni}}(i=1,2) \quad (19)$$

And,

$$A(j\omega)=-\Omega^2+2(\zeta_1+\zeta_2m_r\omega_r)j\Omega+1+{m_r\omega_r}^2$$
$$B(j\omega)=2\zeta_2\omega_rj\Omega+\zeta_2m_r\omega_r$$
$$E(j\omega)=-\Omega^2+2\zeta_2\omega_r(1+c_{32})j\Omega+{\omega_r}^2(1+k_{32}) \quad (20)$$

Based on this simplification, "(16)" can be simplified By, $D_0(j\omega)=k_1^2m_rR(j\Omega)$ where $R(j\Omega)$ can be expressed by,

$$R(j\Omega)=\Omega^4-2j\Omega^3(\zeta_2\omega_r(c_{32}+m_r+1)+\zeta_1)-$$
$$\Omega^2(c_{32}(4\zeta_2^2m_r\omega_r^2+4\zeta_1\zeta_2\omega_r)+k_{32}\omega_r^2+{m_r\omega_r}^2+$$
$$4\zeta_1+\zeta_2\omega_r+{\omega_r}^2+1)+2j\Omega\omega_r(c_{32}(\zeta_2+\zeta_2{m_r\omega_r}^2) \quad (21)$$
$$+\zeta_2+k_{32}(\zeta_2m_r{\omega_r}^2+\zeta_1\omega_r)+\zeta_1\omega_r)+k_{32}m_r\omega_r^4+$$
$$k_{32}\omega_r^2+\omega_r^2$$

where $k_{32}=k_3/k_2$ and $c_{32}=c_3/c_2$

Finally, the frequency response functions, described by "(17)", can be given as,

$$H_{11}(\omega)=k_1\left|\frac{k_1m_rE(j\Omega)}{k_1^2m_rR(j\Omega)}\right|=\left|\frac{E(j\Omega,)}{R(j\Omega)}\right|$$
$$H_{12}(\omega)=k_1\left|\frac{-k_1m_rB(j\Omega)}{k_1^2m_rR(j\Omega}\right|=\left|\frac{B(j\Omega)}{R(j\Omega)}\right| \quad (22)$$

Optimization

In the current work, the modified camel algorithm is used to determine the optimal values of the system parameters that optimize the response of the DVA. The key of using this algorithm is that the dromedary camel has the ability to adjust to extreme heat and prolonged periods of drought, allowing it to live even in situations where there isn't enough water available. There are not enough or low-quality feed resources available. In the winter and other cold seasons, a camel can survive for several months without drinking. It may drink once every 8–10 days during the summer, when dehydration can cause it to lose up to 30% of its body weight. In particular, camels can survive without water for 10–15 days when the mean temperature is between 30 and 35°C, but they need to drink more water for shorter periods of time when the temperature is above 40°C. As they traverse the desert to arrive at their destination, camels have a structured, innate behavior for locating food sources. The camels dispersed throughout a certain area in an attempt to locate the food source. When a particular camel finds a location with plenty of food, it alerts the other camels to that location. The caravan members alter their route in the direction of the food source as long as they can see where that camel is. Food supply location might not be visible to all camels because of the sand dunes in the desert. The camels disappear from view and keep moving randomly in search of more food. While travelling, one camel might come across a better place to eat; in that case, it would notify the other camels to change their course and head in that direction. Until the camels arrive at a specific oasis, this process is continued [34, 35]. Camels move in groups called caravans; they disperse to seek out oases; and when they come across grass, they coordinate with one another to change their course. Some may not be clever to see the grassed area due to the dunes of sand, and move randomly. Another camel may arrive at a better grassed area during this travelling scenario, in which case the updating process is repeated. It is

important to note that during their entire previous journey, the camel caravan searches for the ideal spot. Put differently, the camel caravan modifies its route of travel by considering the optimal location globally instead of locally. It is presumable that a caravan of N camels is traversing a (D) dimensional environment. The vector indicates camel I's location at iteration (iter) $x^{i,iter} = x_1^{i,iter} x_2^{i,iter} x_D^{i,iter}$ where i=1,2,..., N and iter=1,2,..., itermax.

$$x_d^{i,iter} = (x_{max} - x_{min})\,Rand + x_{min} \quad (23)$$

where d is a variable ranging from 1 to D. Word (Rand) is a random number that between 0 and 1. x_{min} and x_{max} represent the minimum limit and the maximum limit of the camel location, respectively. Therefore, the position of each camel is chosen based on a specific fitness function in order to identify the optimal location. The ambient temperature has a direct impact on the locomotion of camels and greatly affects their endurance. As camels migrate to remote areas, they experience varying temperatures, which in turn affects their individual endurance levels. The temperature (T) of camel(i) during time iteration(iter) alters between the minimum T_{min} and maximum T_{max} temperatures as follows:

$$T_d^{i,iter} = (T_{max} - T_{min})\,Rand + T_{min} \quad (24)$$

Temperature effect on the endurance of the camel (E) is presented by:

$$E_d^{i,iter} = 1 - \frac{T_D^{i,iter} - T_{min}}{T_{max} - T_{min}} \quad (25)$$

The presence of sand dunes may obstruct certain vision of the camels, preventing them from rerouting their path to the grassy area that a particular camel has discovered. As a result, two ways are available to update the location of each camel. The update function is provided by when the visibility of a camel (v) exceeds a given value of the visibility threshold:

$$x_D^{i,iter} = x_D^{iter-1} + E_d^{i,iter}(x_d^{best} + x_d^{i,iter-1}) \quad (26)$$

where, according to a particular fitness function, x_d^{best} denotes the best global location, or the best location over all previous iterations. When the visibility(v) is less than the their threshold, the second scenario of the updating process takes place, in which the camel updates its location at random using Eqn (23) [34, 35]. The modified camel algorithm is presented in pseudo code such that [34]:

Begin
Step 1: Initialization: Set the temperature range and the location range T_{min}
and T_{max}; set the camel caravan size and the dimensions; set the visibility threshold; Initialize the location of each camel.
Step 2: Subject the locations to a certain fitness function; determine the current
best location; randomly assign a visibility (v) for each camel.
Step 3: While (iter < itermax) ***do***
for i=1: Camel Caravan size
Compute the temperature T.
Compute the endurance E.
If v < visibility threshold ***then***
Update the camel location.
Else
Update the camel location from.
End If
End for
Subject the new locations to the fitness function
If the new best location is better than the older one
The new best is the global best
End If
Assign new visibility for each camel
Step 4: End While
Step 5: Output the best solution
End

The modified camel algorithm will be used to obtain the optimal design of the DVA presented in this work. In order to determine the best DVA design, the modified camel algorithm is used in conjunction with the negative mass and negative stiffness principles to analyze the dynamic vibration absorber system. From an optimization standpoint, the best curves for these curves are those that minimize the difference between the two upper peaks over a wide range of frequencies and minimize the difference between the two upper peaks and the lower peaks [22, 24, 4, 36, 37]. The algorithm is constraint to achieve the optimized design parameters based on the following constraints:

$$\underset{\zeta_{2w_r}}{Min}\{H_{11}(\Omega uL)\}$$
$$\underset{\zeta_{2w_r}}{Min}\{H_{11}(\Omega uR)\}$$
$$\underset{\zeta_{2w_r}}{Min}\{1/H_{11}(\Omega u)\}$$

Subjected to $w_r \geq 0$ and $\zeta_2 \geq 0$ where ΩuL, ΩuR, Ωu are the frequency of the upper left, upper right, and lower peaks, respectively in the amplitude response $H_{11}(\Omega)$.

3.0 RESULTS AND DISCUSSION

In order to improve absorption capacity and vibration attenuation, the primary goal of this work is to examine the effects of a spring-mass absorber's more sensitive parameters and determine the ideal spring and absorber mass for a unit cell absorber. A detailed discussion of the concepts of negative stiffness and negative mass is given.

1. Negative mass

Effective mass generally varies with absorber mass and excitation frequency. As illustrated in Figure 4, the effective mass indicated by Eqn. (2) turns negative (NM) when $\Omega > \omega_2$. This principle is the key point of using absorber for vibration attenuation that corresponds to $u_1(t) = 0$, as shown by Eqn. (3). On the other hand, when $\Omega < \omega_2$, the effective mass is positive; as a result, both terms $F_0 / a_1 = -\tilde{m}_1 \Omega^2$ and F_0 / a_2 have negative values. Conversely, when the absorber mass increases, the effective mass's absolute value also increases. At higher absorber mass values, though, this increment loses some of its sensitivity.

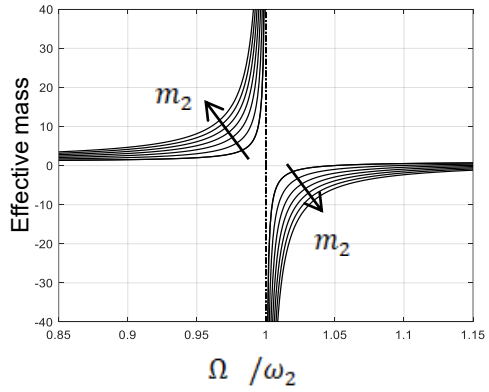

Figure 4 Effective mass with frequency ratio

2. Negative spring

The variation in the effective mass that corresponds to changes in the excitation frequency also affects the effective spring. The frequency ratio is represented by ω_2 / Ω in Figure 5. The spring of the DVA develops a downward force that pushes back against the applied force F(t). In general, the developed force exceeds what is stated in Eqn. (9). The significance of the negative stiffness value for vibration attenuation is explained by this behavior.

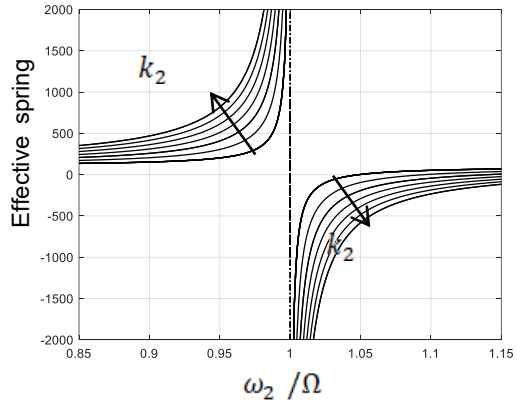

Figure 5 Variations of effective spring due to variation of the frequency ratio

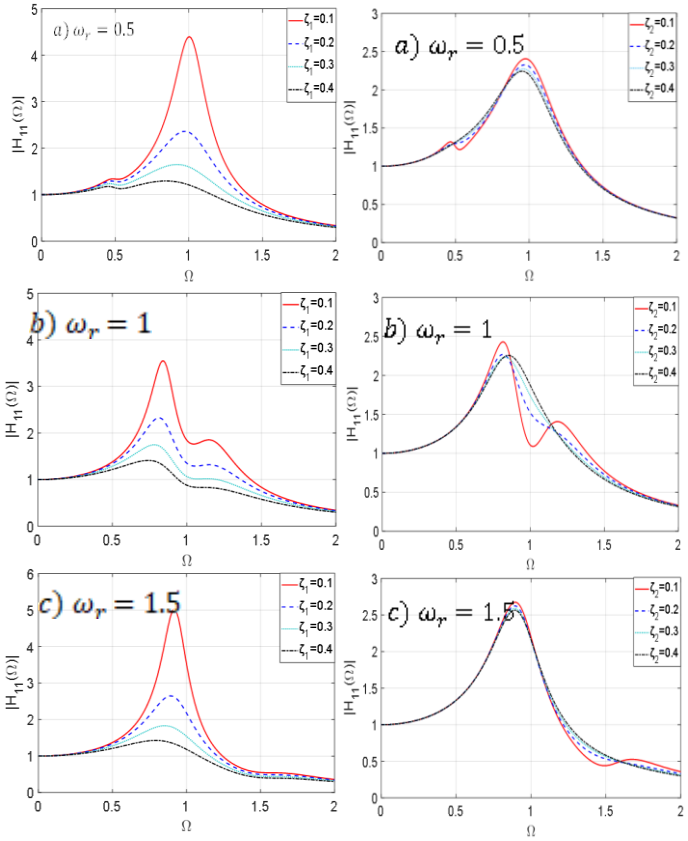

Figure 6 Amplitude responses at $\zeta_2 = 0.2, m_r = 0.1$ for different values of damping ratio and frequency ratio

Figure 7 Amplitude responses at $\zeta_1 = 0.2, m_r = 0.1$ for different values of damping ratio and frequency ratio

An examination is conducted on two absorber designs. There is also research on how sensitive the performance of the absorber performance is to changes in the design parameters. ζ_1 and ζ_2 are assumed to be the damping ratios (DRs) of the primary (main) and DVA system, respectively. The selection of appropriate values and the reduction of the response of the primary vibratory system are crucial components in the design of a good vibration absorber. Making the parameter $a_{22}(j\omega) = 0$ or $R(j\omega) = 0$ when, is the only way to obtain zero response for the primary mass.

3. Arbitrary design

In this design, it is assumed that ($c_3 = k_3 = 0$). Effect of several parameters are studied and explained as follows:

a. Effect of the damping factor ζ_1 on the dynamic response

Figure 6 shows the effect of the first DR for three different frequency ratio values while maintaining a constant mass ratio. Generally speaking, because

both of the introduced DRs are non-zero, no infinite amplitude response is shown. As the DR increase, the amplitude responses drastically decrease. At excitation frequencies smaller than and greater than the first and second resonance frequencies, respectively, the responses are extremely close. But when the frequency ratio increase, the behavior changes. Reducing the amplitude response by 400% involved increasing the DR from (0.1 to 0.4). This means, practically speaking, that systems with higher DRs will experience less vibrations and will avoid resonation damage. In bridge engineering, an increased DR in support systems could help to control vibrations that might arise due to wind or passing vehicles, leading to better structural stability. A higher Dynamic Response (DR) in automotive suspension systems could provide superior ride comfort and increase operational life of system components. In aerospace applications, higher DR in the wings of aircraft could reduce vibrations during flight and improve safety and performance.

b. Effect of damping factor ζ_2 on the dynamic response

Figure 7 illustrates how the three values of frequency ratios cause variations in the amplitude response. As the DR increases, the peaks vanish. As the frequency ratio increases, even peak locations shift. When $\Omega = 1$ and ζ_2 reach their maximum value, the greater effect of ζ_2 is observed. Effect of the DR of the main system is more dominant than that corresponding of the DVA damping ratio, on the dynamic response of the primary system as shown by Figure 6 and Figure 7. However, designing the DVA with suitable values of ζ_2 can control the response of the primary system.

c. Effect of mass ratio on the dynamic response

The impact of mass ratio is presented in Figure 8. The amplitude response changed to be smoother and the peaks gradually vanished when the mass ratio was smaller. But when the frequency ratio equals or exceeds 1, the higher values of the mass ratio peaks become more noticeable and have larger amplitude. It is noteworthy to mention that when (Ω < 0.25), changes in mass ratio and frequency showed no effect on the amplitude response.

d. Effect of frequency ratio on the dynamic response

Figure 9 illustrates how the frequency ratio affects the amplitude response at various mass ratio values. The non-dimensional frequency range (0.5< Ω <1.5) is the range at which the amplitude response changed. Invariant amplitude responses hold true for all other values. Furthermore, the behavioral difference increases sharply as the frequency ratio increases to 1.5 and decreases at lower values of frequency ratio. Practically, in machinery, one can change the frequency ratio to avoid this range so as to not cause too much vibrations, or simply make the machine work better. In structural engineering, knowledge of this correlation is useful to optimize buildings to vibrate less when faced with earthquakes. In aerospace applications, modifying the frequency ratio could help reduce the vibration of wings in airplanes thus improving stability and making flights safer.

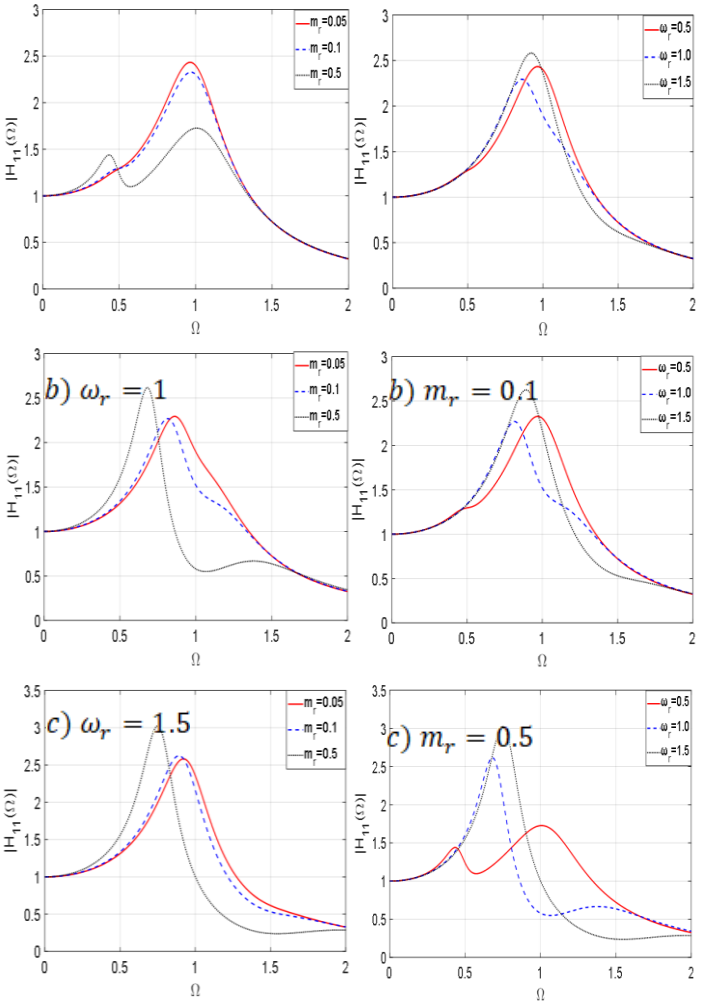

Figure 8 Amplitude response when $\zeta_1 = \zeta_2 = 0.2$ for different values of frequency ratios

Figure 9 Amplitude response when $\zeta_1 = \zeta_2 = 0.2$ for different values of mass ratios

2. Optimal design

When $\zeta_2 = 0$, the time response of the primary mass can be maintain to be zero. This is ideal because of the existence of the structural and frictional damping. Since the absorber performance exhibits nonlinear and fluctuating behavior, selecting the best combinations of system parameters is not an easy task. Figure 10 shows effect of ζ_2 in details, on the amplitude response. When $\Omega = \omega_r = 1$ and $\zeta_2 = 0$ no response. Other than that, though, the behavior is different where the peaks of the amplitude response

decrease. However, both peaks ($\Omega \neq 0$) go to infinity when $\zeta_2 = 0$ and $\zeta_2 = \infty$.

Put differently, there exists a critical value of ζ_2, at which the peaks attain their minimum or smaller size. The best behavior for these curves, in terms of optimization, is exhibited by curves that minimize the difference between the two upper peaks in the frequency response over a broad range of non-dimensional frequencies, and make the difference between the two upper peaks and the lower peaks as small as possible [22, 24, 4, 36, 37]. In order to determine the best DVA design [39-42], the modified camel algorithm is used in conjunction with the negative mass and negative stiffness principles to analyze the dynamic vibration absorber system.

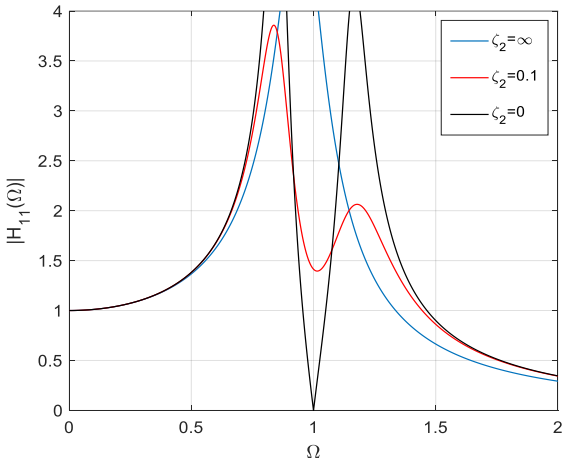

Figure10 Nonlinear effect of damping

The algorithm as stated in Table 1 is validated by comparing the outcomes with multiple references. In addition, the current algorithm is efficient [43-46] and faster in CPU time than the other methods used in the references.

Table 1 Optimal value of the critical design parameters

Ref. No.	ω_r	ζ_2	CPU time
Current work	**0.8615**	**0.215**	**159 sec**
[4]	**0.861**	**0.204**	**N/A**
[24]	**0.909**	**0.185**	**N/A**
[36]	**0.861**	**0.202**	**568.5 sec**
[37]	**0.862**	**0.199**	**N/A**
[38]	**0.862**	**0.197**	**409.5 sec**

The results in Figure 11 show a clear improvement in amplitude responses. The dashed line represents the current work, which outperforms the references in Table 1. The camel algorithm achieves nearly all three constraints, indicating strong effectiveness. A key takeaway from this figure is the minimized differences between peaks compared to earlier studies. This indicates that the current methodology not only competes well but also improves precision in meeting specifications. The visual representation highlights how this approach consistently aligns more closely with desired responses than the alternatives.

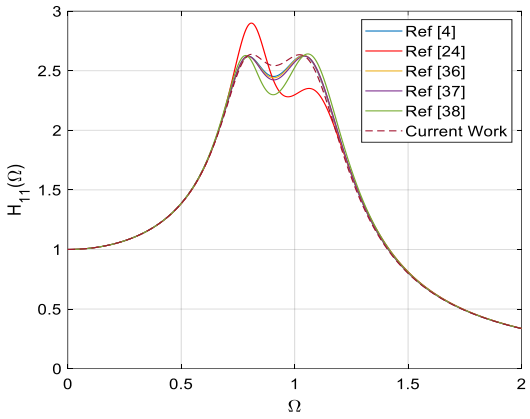

Figure 11 Comparison of amplitude response for different optimized DVA designs

4.0 CONCLUSION

The concepts of negative mass and negative springs were presented and thoroughly examined in order to design a dynamic absorber. The best DVA design is obtained by applying the modified camel algorithm. The results showed how crucial DRs and frequency response are to the creation of a successful dynamic absorber. When $\zeta_2 = 0$, the primary mass can reach zero response. There exists a critical value at which the peaks attain their minimum or smaller size. Changes in the mass ratio and frequency have no effect on the amplitude response when $\Omega < 0.25$. The response is only impacted by frequency ratio in the range of ($0.5 < \Omega < 1.5$). In comparison to previous works, the modified camel algorithm demonstrated faster convergence to DVA response constraints and better optimized values of DVA parameters.

Acknowledgement

Authors would like to thank both of Al-Mustaqbal Universoty, Al-Mustaqbal Energy Research Center, Hilla/Iraq, and University of Babylon, /Hilla/Iraq for their supports.

Conflicts of Interest

The authors declare that there is no conflict of interest regarding the publication of this paper.

References

[1] Frahm, H. 1909. Device for Damping Vibrations of Bodies. U.S. Patent 989,958.

[2] Frahm, H. 1911. Device for Damping Vibrations of Bodies. U.S. Patent 989,958.

[3] Snowdon, J. C. 1968. *Vibration and Shock in Damped Mechanical Systems*. New York: Wiley.

[4] Randall, S. E. 1981. Optimum Vibration Absorbers for Linear Damped Systems. *Journal of Mechanical Design*. 103: 908–913.

[5] Zuo, L., and S. A. Nayfeh. 2004. Minimax Optimization of Multi-Degree-of-Freedom Tuned-Mass Dampers. *Journal of Sound and Vibration*. 272: 893–908.

[6] Fortgang, J., and W. Sinhose. 2005. Design of Vibration Absorbers for Step Motion and Step Disturbances. *Transactions of the ASME*. 127: 160–163.

[7] Liu, K., and G. Coppola. 2010. Optimal Design of Damped Dynamic Vibration Absorber for Damped Primary Systems. *Transactions of the Canadian Society for Mechanical Engineering*. 34: 119–135.

[8] Liu, K., and J. Liu. 2005. The Damped Dynamic Vibration Absorbers: Revisited and New Result. *Journal of Sound and Vibration*. 284: 1181–1189.

[9] Zuo, L., and S. A. Nayfeh. 2006. The Two-Degree-of-Freedom Tuned-Mass Damper for Suppression of Single-Mode Vibration under Random and Harmonic Excitation. *Transactions of the ASME*. 128: 56–65.

[10] Ghosh, A., and B. Basu. 2007. A Closed-Form Optimal Tuning Criterion for TMD in Damped Structures. *Structural Control and Health Monitoring*. 14: 681–692.

[11] Wong, W. O., and Y. Cheung. 2008. Optimal Design of a Damped Dynamic Vibration Absorber for Vibration Control of Structure Excited by Ground Motion. *Engineering Structures*. 30: 41–46.

[12] Viana, F. A. C., D. A. Kotinda, and V. Rade, *et al*. 2008. Tuning Dynamic Absorbers by Ant Colony Optimization. *Computer Methods in Applied Mechanics and Engineering*. 86: 1539–1549.

[13] Lakes, R. S. 2001. Extreme Damping in Composite Materials with a Negative Stiffness Phase. *Physical Review Letters*. 86(13): 2897–2900.

[14] Lakes, R. S. 2001. Extreme Damping in Compliant Composites with a Negative-Stiffness Phase. *Philosophical Magazine Letters*. 81(2): 95–100.

[15] Lakes, R. S., T. Lee, A. Bersie, and Y. C. Wang. 2001. Extreme Damping in Composite Materials with Negative-Stiffness Inclusions. *Nature*. 410(6828): 565–567.

[16] Lakes, R. S., and W. J. Drugan. 2002. Dramatically Stiffer Elastic Composite Materials Due to a Negative Stiffness Phase? *Journal of the Mechanics and Physics of Solids*. 50(5): 979–1009.

[17] Wang, Y. C., and R. S. Lakes. 2004. Extreme Stiffness Systems Due to Negative Stiffness Elements. *American Journal of Physics*. 72(1): 40–50.

[18] Wang, Y. C., and R. S. Lakes. 2004. Negative Stiffness-Induced Extreme Viscoelastic Mechanical Properties: Stability and Dynamics. *Philosophical Magazine*. 84(35).

[19] Wang, Y. C., and R. S. Lakes. 2005. Stability of Negative Stiffness Viscoelastic Systems. *Quarterly of Applied Mathematics*. 63(1): 34–55.

[20] Platus, D. L. 1992. Negative-Stiffness-Mechanism Vibration Isolation Systems. *Proceedings of SPIE*.

[21] Mizuno, T., T. Toumiya, and M. Takasaki. 2003. Vibration Isolation System Using Negative Stiffness. *JSME International Journal Series C*. 46(3): 807–812.

[22] Acar, M. A., and C. Yilmaz. 2013. Design of an Adaptive–Passive Dynamic Vibration Absorber Composed of a String–Mass System Equipped with Negative Stiffness Tension Adjusting Mechanism. *Journal of Sound and Vibration*. 332(2): 231–245.

[23] Yang, J., Y. Xiong, and J. Xing. 2013. Dynamics and Power Flow Behaviour of a Nonlinear Vibration Isolation System with a Negative Stiffness Mechanism. *Journal of Sound and Vibration*. 332(1): 167–183.

[24] Den Hartog, J. P. 1981. *Mechanical Vibrations*. New York: Courier Corporation.

[25] Yang, F., R. Sedaghati, and E. Esmailzadeh. 2022. Vibration Suppression of Structures Using Tuned Mass Damper Technology: A State-of-the-Art Review. *Journal of Vibration and Control*. 28(7–8): 812–836.

[26] Li, C., and B. Zhu. 2006. Estimating Double Tuned Mass Dampers for Structures under Ground Acceleration Using a Novel Optimum Criterion. *Journal of Sound and Vibration*. 298 (1–2): 280–297.

[27] Lee, C. L., Y. T. Chen, L. L. Chung, and Y. P. Wang. 2006. Optimal Design Theories and Applications of Tuned Mass Dampers. *Engineering Structures*. 28(1): 43–53.

[28] Zuo, L., and S. A. Nayfeh. 2005. Optimization of the Individual Stiffness and Damping Parameters in Multiple-Tuned-Mass-Damper Systems. *Journal of Vibration and Acoustics*. 127(1): 77–83.

[29] Hoang, N., and P. Warnitchai. 2005. Design of Multiple Tuned Mass Dampers by Using a Numerical Optimizer. *Earthquake Engineering & Structural Dynamics*. 34(2): 125–144.

[30] Rao, S. S. 1996. *Engineering Optimization: Theory and Practice*. New York: John Wiley and Sons.

[31] Hadi, M. N. S., and Y. Arfiadi. 1998. Optimum Design of Absorber for MDOF Structures. *Journal of Structural Engineering*. 124(11): 1272–1280.

[32] Febbo, M., and S. A. Vera. 2008. Optimization of a Two Degree of Freedom System Acting as a Dynamic Vibration Absorber. *Journal of Vibration and Control*. 14(11): 1667–1683. https://doi.org/10.1177/1077546307081586.

[33] Park, J., and D. Reed. 2001. Analysis of Uniformly and Linearly Distributed Mass Dampers under Harmonic and Earthquake Excitation. *Engineering Structures*. 23: 802–814.

[34] Ali, R. S., T. B. Abbass, and others. 2019. A Modified Camel Travelling Behaviour Algorithm for Engineering Applications. *Australian Journal of Electrical and Electronics Engineering*. 16(3): 176–186.

[35] Alnahwi, F. M., Y. I. A. Al-Yasir, D. Sattar, R. S. Ali, C. H. See, and R. A. Abd-Alhameed. 2021. A New Optimization Algorithm Based on the Fungi Kingdom Expansion Behavior for Antenna Applications. *Electronics*. 10: 2057. https://doi.org/10.3390/electronics10172057.

[36] Brown, B., and T. Singh. 2010. Minimax Design of Vibration Absorbers for Linear Damped Systems. *Journal of Sound and Vibration*. 330: 2437–2448.

[37] Randall, S. E. 1981. Optimum Vibration Absorbers for Linear Damped Systems. *Journal of Mechanical Design*. 103: 908–913.

[38] Fang, J., S. Shi-Min, and Q. Wang. 2012. Optimal Design of Vibration Absorber Using Minimax Criterion with Simplified Constraints. *Acta Mechanica Sinica*. 28(3): 848–853.

[39] Abbass, T. B., S. O. W. Khafaji, M. Al-shujairi, and M. J. Aubad. 2025. Experimental Evaluation of the Performance of Dynamic Vibration Absorbers for Vibration Mitigation in Beam Structures. *Jurnal Teknologi (Sciences & Engineering)*. 87(1): 159–166.

[40] Jabbar, F. A., P. S. Rao, and S. O. W. Khafaji. 2024. Enhancing the Design of Dynamic Vibration Absorbers through Harmonic Analysis and Lumped Parallel Configuration. *Engineering, Technology & Applied Science Research*. 14(5): 16624–16639.

[41] Abbas, T. B., and S. O. W. Khafaji. 2024. Experimental Evaluation of Dynamic Vibration Absorbers for Vibration Suppression in Beam Structure. In *AIP Conference Proceedings*. 3097(1). AIP Publishing.

[42] Jabbar, F. A., P. S. Rao, and S. O. W. Khafaji. 2024. Reducing Vibration Amplitude with Parametric Optimization and an Efficient Dynamic Vibration Absorber for a Supported Beam. *The Iraqi Journal for Mechanical and Materials Engineering*. 23(2): 76–102.

[43] Al-mtory, H. A., F. M. Alnahwi, and R. S. Ali. 2024. A New Algorithm Based on Pitting Corrosion for Engineering

Design Optimization Problems. *Iraqi Journal for Electrical and Electronic Engineering*. 20(2): 190–206.
[44] Ali, R., J. Mahmood, and H. Badr. 2022. A New Version of Modified Camel Algorithm for Engineering Applications. In *Proceedings of the 2nd International Multi-Disciplinary Conference*, Sakarya, Turkey.
[45] Utama, D. M., W. N. Safitri, and A. K. Garside. 2022. A Modified Camel Algorithm for Optimizing Green Vehicle Routing Problem with Time Windows. *Jurnal Teknik Industri*. 24(1): 23–36.
[46] Al-mtory, H. A., F. M. Alnahwi, and R. S. Ali. 2024. Beamforming Optimization of Linear and Planar Antenna Array Using a New Algorithm Based on the Corrosion Diffusion Behavior. *Arabian Journal for Science and Engineering*. 49(12): 16959–16984.